

Controlling the Fluorescence Properties of Nitrogen Vacancy Centers in Nanodiamonds

Christian Laube,^{a,b} Thomas Oeckinghaus,^c Jan Lehnert,^a Jan Griebel,^a Wolfgang Knolle,^a Andrej Denisenko,^c Axel Kahnt,^a Jan Meijer,^d Jörg Wrachtrup,^c Bernd Abel^{a,b,*}

^a Leibniz-Institute of Surface Engineering (IOM), Permoserstr. 15, D-04318 Leipzig, Germany, bernd.abel@iom-leipzig.de, axel.kahnt@iom-leipzig.de

^b Wilhelm-Ostwald-Institute for Physical and Theoretical Chemistry, University of Leipzig, Linnéstraße 2, 04103 Leipzig

^c Institute of Physics, Research Centre SCoPE and IQST, University of Stuttgart, 70569 Stuttgart, Germany.

^d Faculty of Physics and Earth Sciences, Felix Bloch Institute for Solid State Physics, Leipzig University, Linnéstraße 5, 04103 Leipzig, Germany

Table of Contents

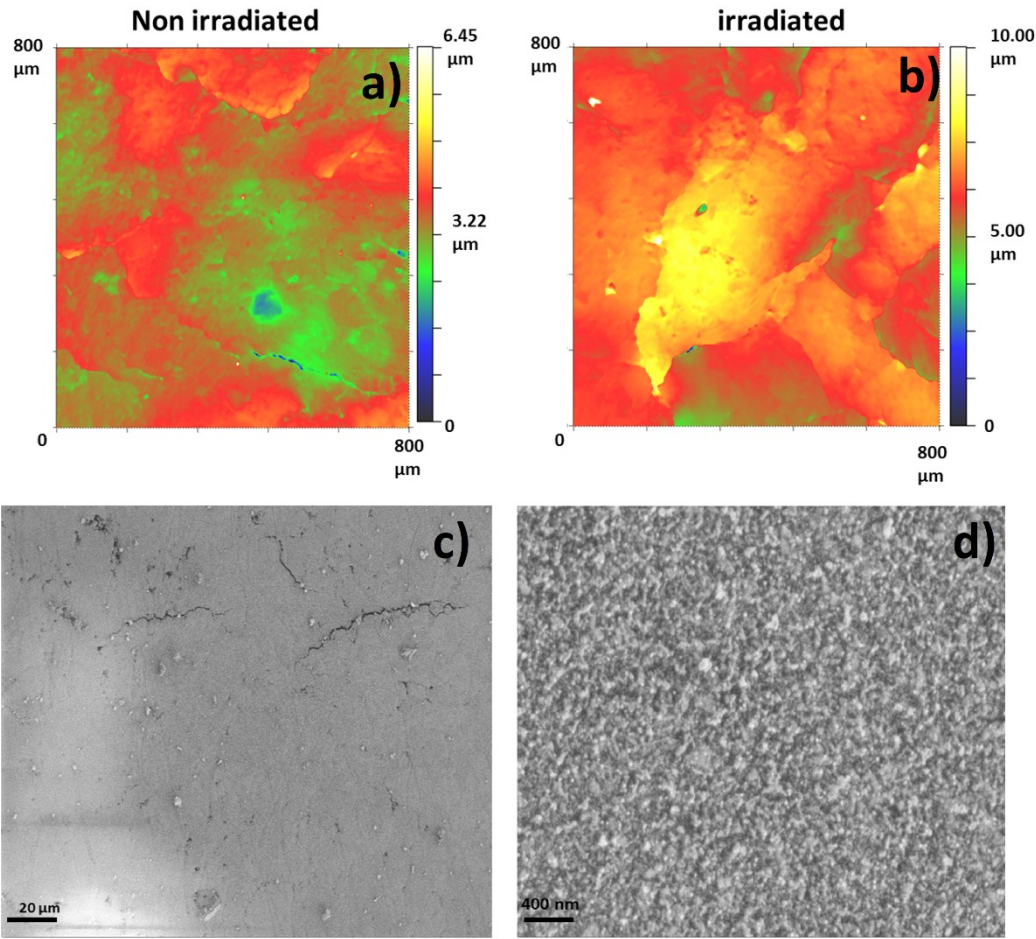
Pellet surface morphology and particle surface functionality investigations for OND containing pellets	S3
Profilometry and Scanning Electron Microscopy Images of ND Pellets	S4
Attenuated-Total-Reflection-Infrared-Spectroscopy (ATR-IR) of OND after different Treatments	S5
X-ray Photoelectron Spectroscopy (XPS) of OND after different treatments	S6
Ray Diffractogram of OND	S7
Effect of irradiation induced lattice defects on the fluorescence properties of NV center	S8
Fluorescence Lifetime investigations	S11
Parameter study of the used FLIM-setup	S14
FLIM investigations of HF treated OND (Silica free sample)	S15
Fluorescence lifetime and intensity to fluence dependency	S16
Single particle investigations for NV center Content Evaluation	S17
Particle surface functionality effect on fluorescence properties of NV center	S18
ATR-IR spectra of the investigated NDs with different Surface Terminations	S20
Fluorescence-Lifetime Images of Pellets of NDs with different Surface Terminations	S21

**Pellet surface morphology and particle surface functionality investigations for
OND containing pellets**



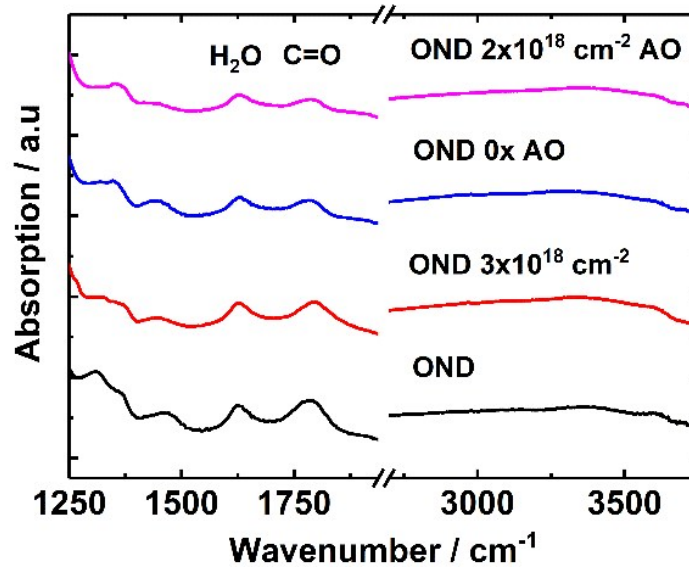
S11 Image of ND pellets after first air etching (left), directly after irradiation (middle), after irradiation and post-treatment.

Profilometry and Scanning Electron Microscopy Images of ND Pellets



S12 Representative profilometry image of: **a)** non-treated **b)** irradiated and post-treated OND pellets, **c)** Scanning electron microscopy images (SEM) of the surface of OND-pellet irradiated and post-treatment OND-pellet, **d)** higher resolution SEM-image of **c**.

Attenuated-Total-Reflection-Infrared-Spectroscopy (ATR-IR) of OND after different Treatments



S13 ATR-IR-spectra of OND after different treatment step **Black:** OND without additional treatment, **Red:** OND irradiated without annealing and second oxidation, **Blue:** OND non-irradiated with post-treatment, **Magenta:** OND irradiated ($\Phi = 2 \cdot 10^{18} \text{ cm}^{-2}$) with post-treatment.

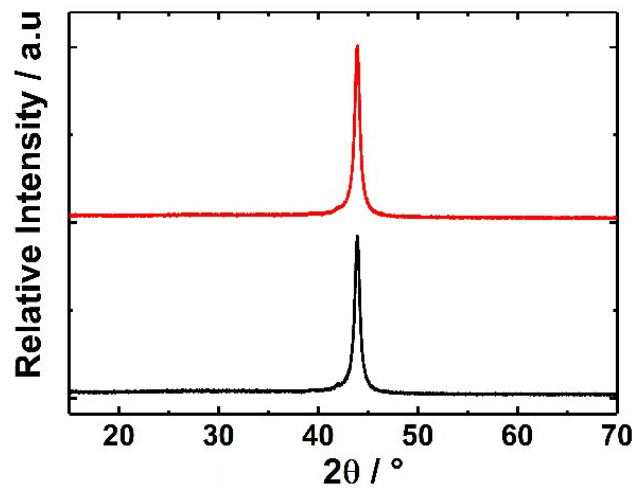
X-ray Photoelectron Spectroscopy (XPS) of OND after different treatments

T1 XPS results element analysis

Atom content (SiO ₂ corrected)	OND	OND irradiation	OND + post- treatment	OND irradiation + post- treatment
C [%]	84.1	85.8	87.8	86.4
O [%]	15.9	14.3	12.2	13.6

According to the ATR and XPS results our irradiation and post-treatment conditions lead to a reproducible reduction of the surface of the ND. So the observed ATR-IR spectra illustrate a decrease of the peak at 1780 cm⁻¹ in relation to the peak at 1620 cm⁻¹. The peak at 1780 cm⁻¹ can be related to the carbonylic and carboxylic groups, whereas the peak at 1620 cm⁻¹ belongs to water shell on the diamond surface.¹ The decrease of the 1780 cm⁻¹ peak therefore indicates the reduction of highly oxidized surface functionality on the ND surface. This result is confirmed by the reduced oxygen atom percentage detected by XPS. The approach of the atom percentage calculation is described elsewhere.²

X-Ray Diffractogram of OND



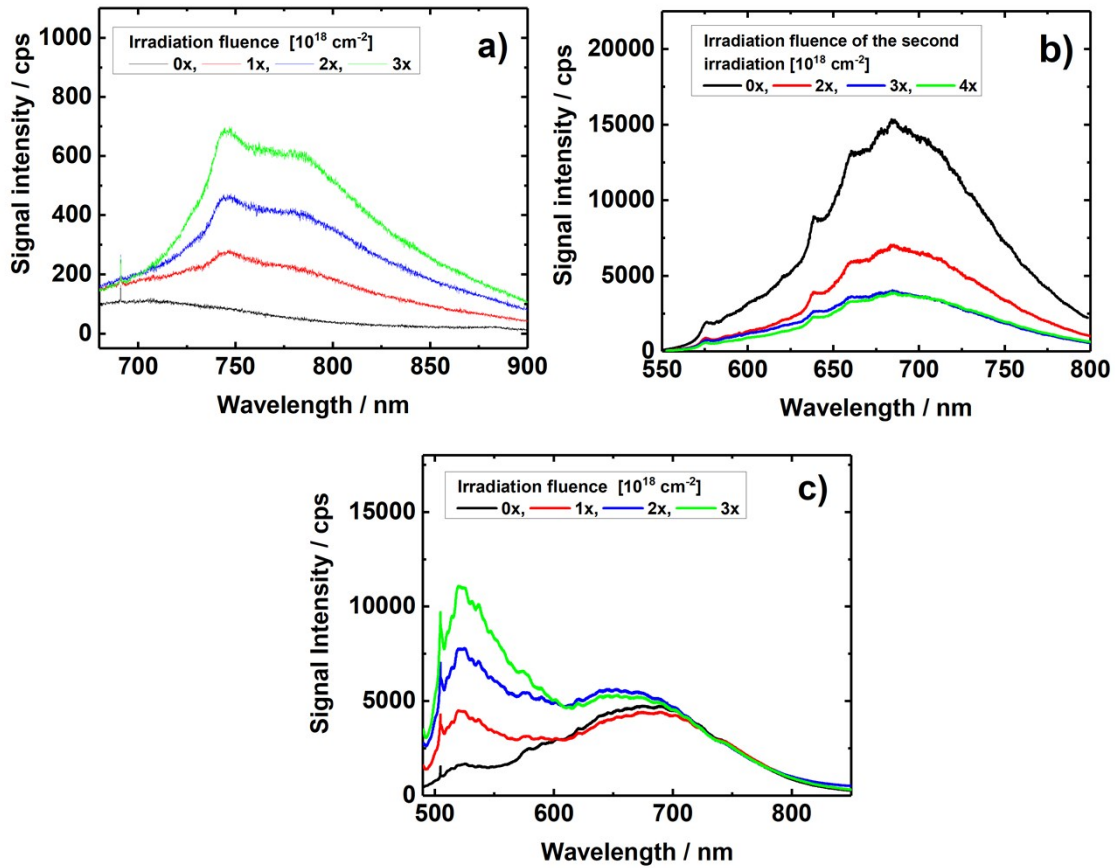
S15 X-Ray diffractogram of OND **Red:** without irradiation and post-treatment, **Black:** after irradiation ($\Phi = 2 \cdot 10^{18} \text{ cm}^{-2}$) and post-treatment (black).

Within the detected X-Ray diffractograms before and after irradiation and post-treatment no graphite related signals are observable indicating the purity of the investigated ND samples.

Effect of irradiation induced lattice defects on the fluorescence properties of NV center

Steady state investigation

To monitor the vacancy generation during the irradiation the GR1 center fluorescence related to neutrally charged Frenkel defects was investigated directly after irradiation without any post-treatment.³ This study not only provides a quality control of the irradiation process before annealing, it also enable us to study the influences of GR1 to the NV center that could provide an easy tunable, controllable and reproducible way to manipulate the optical properties of the NV centers. According to *Jelezko et al.* the GR1 center has a low fluorescence lifetime (FL) about 1 ns and quantum yield of 0.01.⁴ As illustrated in figure SI6a the spectra of the GR1 center fluorescence spectra overlaps with the NV⁻ center. With increasing irradiation the characteristic spectra of the GR1 center with a ZPL at 740 nm is quiet good observable. The enhancement of the GR1 center related fluorescence follows a linear trend for fluence up to $3 \cdot 10^{18} \text{ cm}^{-2}$ (figure SI6a-c). Due to the absence of a graphite related unspecific fluorescence we can conclude that we do not destroy the diamond during irradiation. On the other hand the results show that we are still not at a saturation region for the vacancy formation. This fact is important as it indicates the saturation of NV production is not vacancy related, and thus, the accessibility of single nitrogen seems to be the limiting factor for NV center generation insight the ND.



SI6 Effect of irradiation on NV center fluorescence properties: **a)** Fluorescence spectra upon excitation with 633 nm of OND irradiated with different fluences without post-treatment; **b)** Fluorescence spectra upon excitation with 532 nm of OND irradiated with $\Phi = 2 \cdot 10^{18} \text{ cm}^{-2}$ with post-treatment followed by a second irradiation with different fluences **c)** Fluorescence spectra upon excitation with 473 nm of OND irradiated with different fluences without post-treatment (normalized at 740 nm).

With increasing irradiation fluence we also observed a quenching of the NV center fluorescence. The quenching becomes even more distinct if the NV center content in the ND is increased (see SI6b). In addition, a small increase of the NV^- to NV^0 ratio with increasing fluence which follows no significant trend occurs. Note that because of the absence of post-treatment the surface functionality of the irradiated samples can differ from the non-irradiated sample during this experiment. We consider these small surface functionality changes as the origin of the NV^- to NV^0 ratio changes. The quenching of NV center fluorescence quenching may have many possible origins such as lattice stress, surface changes or additional color center interactions. In literature different forms of lattice damage related color center after irradiation were described such as the TR12 and 3H center.^{5,6} Consequently, we cannot

directly relate the quenching of the NV center to the GR1, even if the necessary overlap of the GR1 absorption band with the NV center fluorescence band is given.⁷ To proof the quenching behavior of the GR1 we performed experiments where we excite only the NV center using 473 nm excitation wavelength (SI6c). In case of an energy transfer from NV center to GR1 center one would expect the GR1 fluorescence even without direct excitation. However, the observed fluorescence spectra show no significant formation of the GR1 center related fluorescence spectra but a strong fluorescence band in the range of 500 nm to 575 nm with a ZPL at 503 nm which is typical for a 3H center (SI6c).⁸

Manfredotti et al. demonstrate a decrease of NV⁰ fluorescence in conjunction with an increase of 3H center content⁵. Nevertheless, a direct proof of a quenching NV center by means of energy transfer from the NV center to an irradiation induced color center is still not confirmed. So an irradiation induced non-fluorescent color center could also be quenching relevant as **Deák et al.** pointed out by showing the effects of di-vacancies on the formation on NV⁻ centers based on non-local hybrid density functional supercell plane wave calculations.⁹ We need further investigations to get more insight into the complex quenching system.

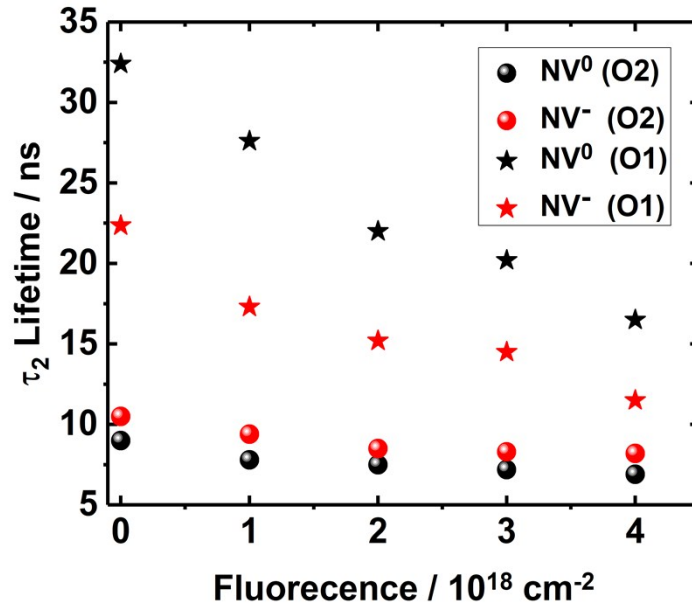
We also want to point out that during the annealing step the system totally change by converting irradiation damages and thus the quenching of NV by irradiation damage has a secondary relevance in terms of optimizing the NV fluorescence intensity.

Fluorescence Lifetime investigations

As described in the steady state part we observed changes of the NV center properties by producing irradiation damage during a second irradiation without post-treatment. To study these effects we also investigated the electron fluence dependency on the dynamical fluorescence properties of the NV center. Figure S17 illustrates the effect of the second irradiation to the τ_2 -FL of a previously irradiated and post-treated sample and a sample without previous irradiation. For both samples a significant decrease of the τ_2 for all charge states can be observed. The curve progression can be described as a linear relation that is followed by a saturation behavior at fluences higher than $\Phi = 3 \cdot 10^{18} \text{ cm}^{-2}$. The saturation can be explained by the limited accessibility of NV center in case of too high vacancy concentrations. By assuming that the quenching due to irradiation damage follows linear FL to fluence dependence up to $\Phi = 3 \cdot 10^{18} \text{ cm}^{-2}$ we investigated a Stern-Volmer-Plot to achieve the resulting quenching constant using equation 1.

$$\frac{1}{\tau_{fluence}} = k_Q * [Q] + \frac{1}{\tau_0} \quad (1)$$

Where $\tau_{fluence}$ is the fluence dependent FL, [Q] is the quencher concentration due to irradiation damage, τ_0 is the radiative lifetime, i.e. the FL in absence of the quencher and k_Q is the quenching constant for the quenching process. Normally, the Stern-Volmer equation is used for dynamical quenching systems but since the distance of the quencher to NV center is within the range of 10 nm this approximation becomes reasonable. The plot was performed for the previous irradiated and post-treated samples after second irradiation without post-treatment (O1) and samples that were irradiated without post-treatment (O2). We observed the changes of both transients τ_1 and τ_2 . For the obtained values we want to emphasize that side effects due to the overlap with different color center e.g. GR1 and 3H could not be separated during these experiments. Also an interaction effect with residual C center needs to be considered in case of O2. The results are listed in table 1. The data display two trends: first a higher quenching constant for τ_1 compared to τ_2 and second different trend of the quenching constant depending on the charge state comparing O2 ($k_Q(NV^0) > k_Q(NV^-)$) and O1 ($k_Q(NV^0) < k_Q(NV^-)$).



S17 Quenching effect of irradiation fluence (without post-treatment) on already existing NV center **black:** NV⁰, **red:** NV⁻, **dots:** irradiated sample without post-treatment, **stars:** irradiated ($2 \cdot 10^{18} \text{ cm}^{-2}$) and post-treated OND with additional irradiation fluence without post-treatment.

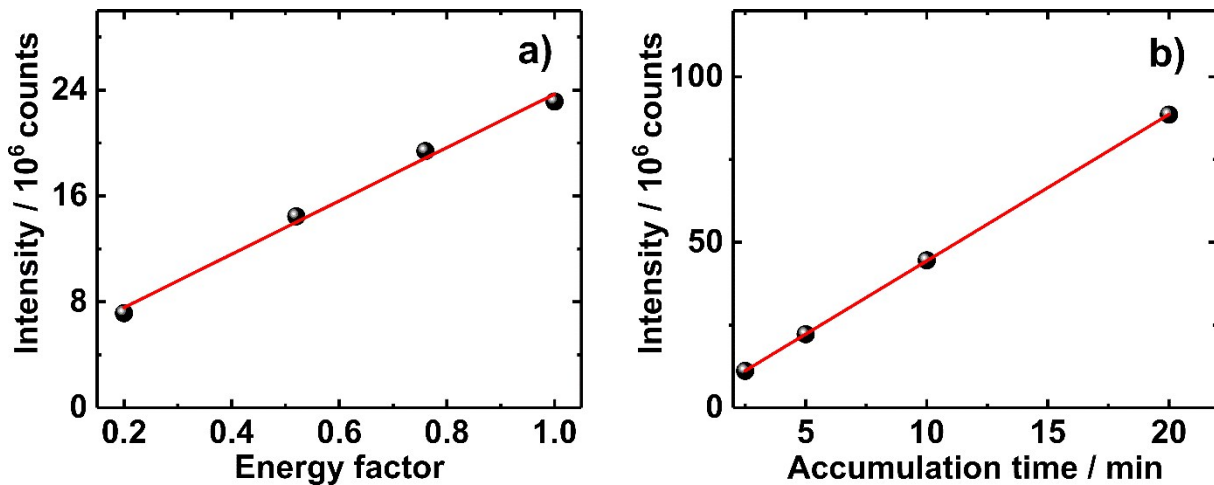
Table 1 quenching parameter for quenching due to irradiation induce lattice defects

	$\tau_0(\text{O2})$ [ns]	$k_Q(\text{O2})$ [1/ns * 10 ¹⁸ cm ⁻²]	$\tau_0(\text{O1})$ [ns]	$k_Q(\text{O1})$ [1/ns * 10 ¹⁸ cm ⁻²]
$\tau_1(\text{NV}^0)$	1.05 ± 0.10	0.123 ± 0.04	2.24 ± 0.33	0.056 ± 0.024
$\tau_1(\text{NV}^-)$	0.87 ± 0.03	0.064 ± 0.02	2.00 ± 0.10	0.082 ± 0.008
$\tau_2(\text{NV}^0)$	8.70 ± 0.20	0.0078 ± 0.0013	32.70 ± 2.00	0.0071 ± 0.0010
$\tau_2(\text{NV}^-)$	10.50 ± 0.30	0.0068 ± 0.0014	22.60 ± 2.00	0.0099 ± 0.0018

The second effect may originate from several different effects. First the overlapping with the GR1 center fluorescence needs to be considered even if the reported fluorescence quantum yield of the GR1 center is reported to be low. Also an additional increase of the quenching efficiency of the quenching environment of τ_1 due to irradiation induced defect is reasonable. Consider nitrogen cluster as quenching environment the irradiation effect could lead to

changes of the C center cluster energy level improving the overlap to the NV center energy level. If we now assume τ_1 originates from NV centers close to many C centers we could explain both the higher quenching rate and the more distinct inversion of quenching efficiency in terms of the charge state by means of irradiation. Nevertheless, this assumption needs to be proven by experiments with different nitrogen content that will be the subject of future work.

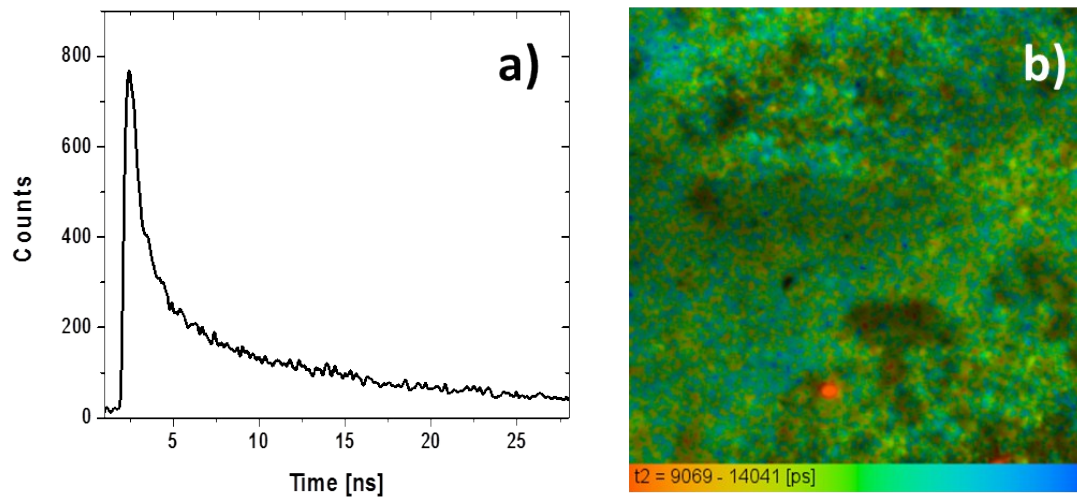
Parameter study of the used FLIM-setup



S18 Parameter dependence of the intensity of an OND sample ($\Phi = 2 \cdot 10^{18} \text{ cm}^{-2}$, with post-treatment) detected by FLIM based relative intensity approach: **a)** Laser energy variation Energy factor corresponds to the laser energy used for all experiments accumulation time 5 minutes; **b)** Accumulated counts for different accumulation times.

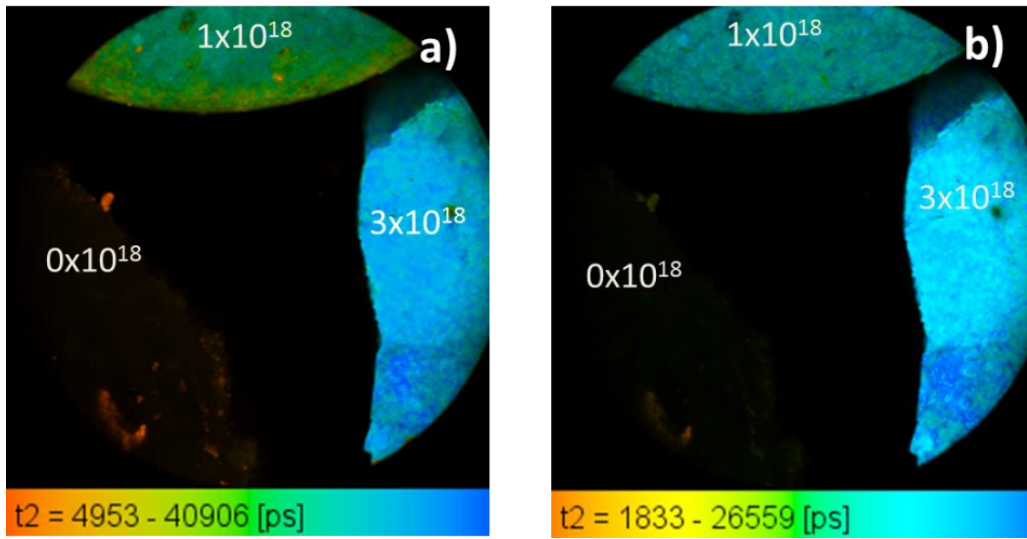
For the FLIM approach several error sources like bleaching of the sample, laser instability, death time (including pile up) or saturation effects of the detector need to be considered. So experiments were performed to exclude these error sources. To exclude the death time and saturation caused errors we tested the intensity behavior of a set of samples using different grey filter level which reduces the fluorescence intensity of the high fluence sample ($\Phi = 3 \cdot 10^{18} \text{ cm}^{-2}$) to the optimum scan level of the detector (10^5 photons/s, less than 0.5 % of the excitation photon rate). As the trend of the results was similar to the results with regular grey filter level conditions, we can exclude the death time as error source. A variation of the accumulation time shows a linear trend of the intensity demonstrating good laser stability and no bleaching occurs using the chosen experimental parameter. Changes of the fluorescence intensity according to varied laser intensity also follow a linear behavior (S18). Derived from these experiments most technical errors sources can be excluded. Therefore, changes of the fluorescence intensity can be related to changes of NV center amount and their fluorescence properties.

FLIM investigations of HF treated OND (Silica free sample)



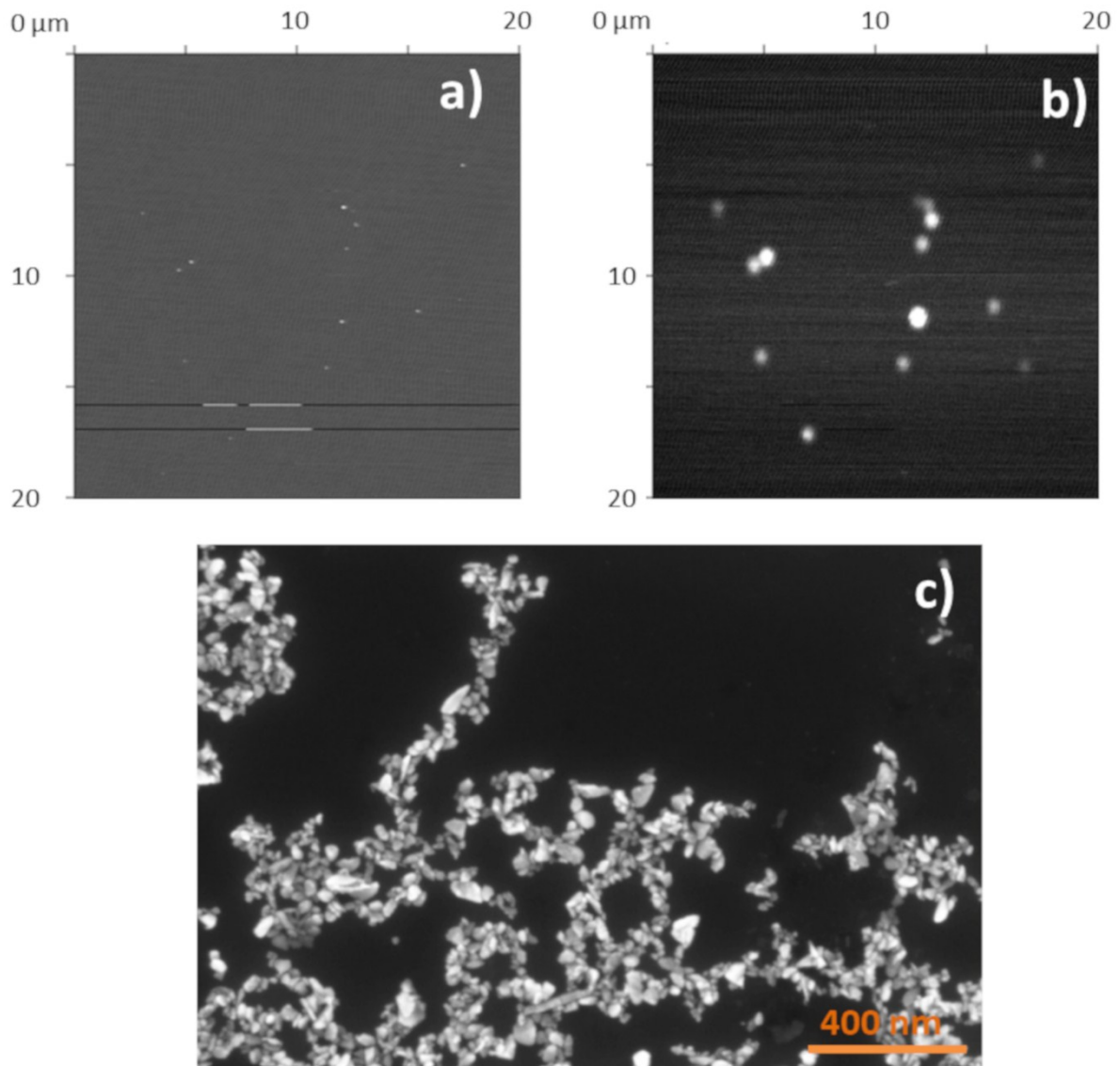
S19 FLIM investigations of HF treated OND: **a)** time profile of HF treated OND without irradiation and post-treatment upon 513 nm excitation, **b)** FLIM image for τ_2 -transient.

Fluorescence lifetime and intensity to fluence dependency



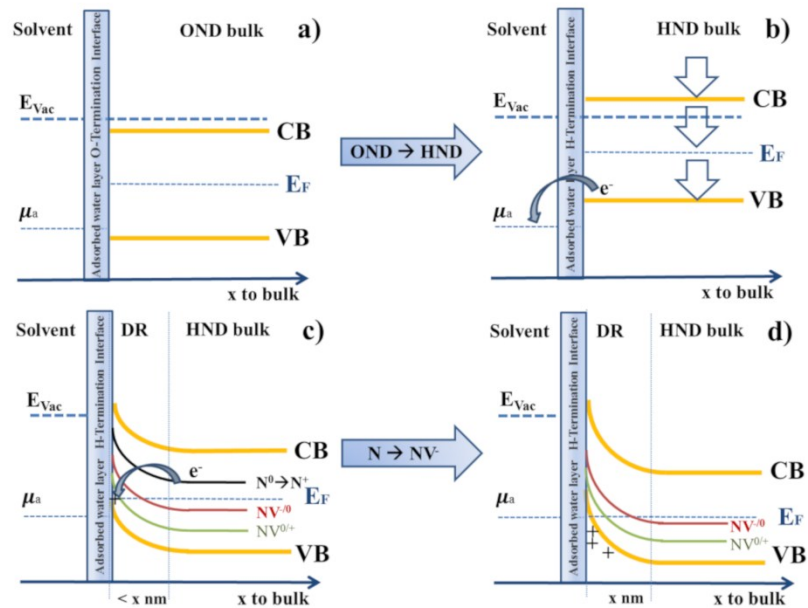
S110 FLIM image $\lambda_{\text{ex}} = 514$ nm of OND pellets irradiated with different fluences, circle image section with diameter of 1.85 mm: **a)** FLIM-image of NV⁰-channel; **b)** FLIM-image of NV⁻channel.

Single particle investigations for NV center Content Evaluation



S111 Representative image of the sample investigated with the AFM-coupled-Antibunching measurements: **a)** AFM-map; **b)** fluorescence image; **c)** SEM-image of a different sample prepared with identical treatment parameter as the sample observed in a and b.

Particle surface functionality effect on fluorescence properties of NV centre

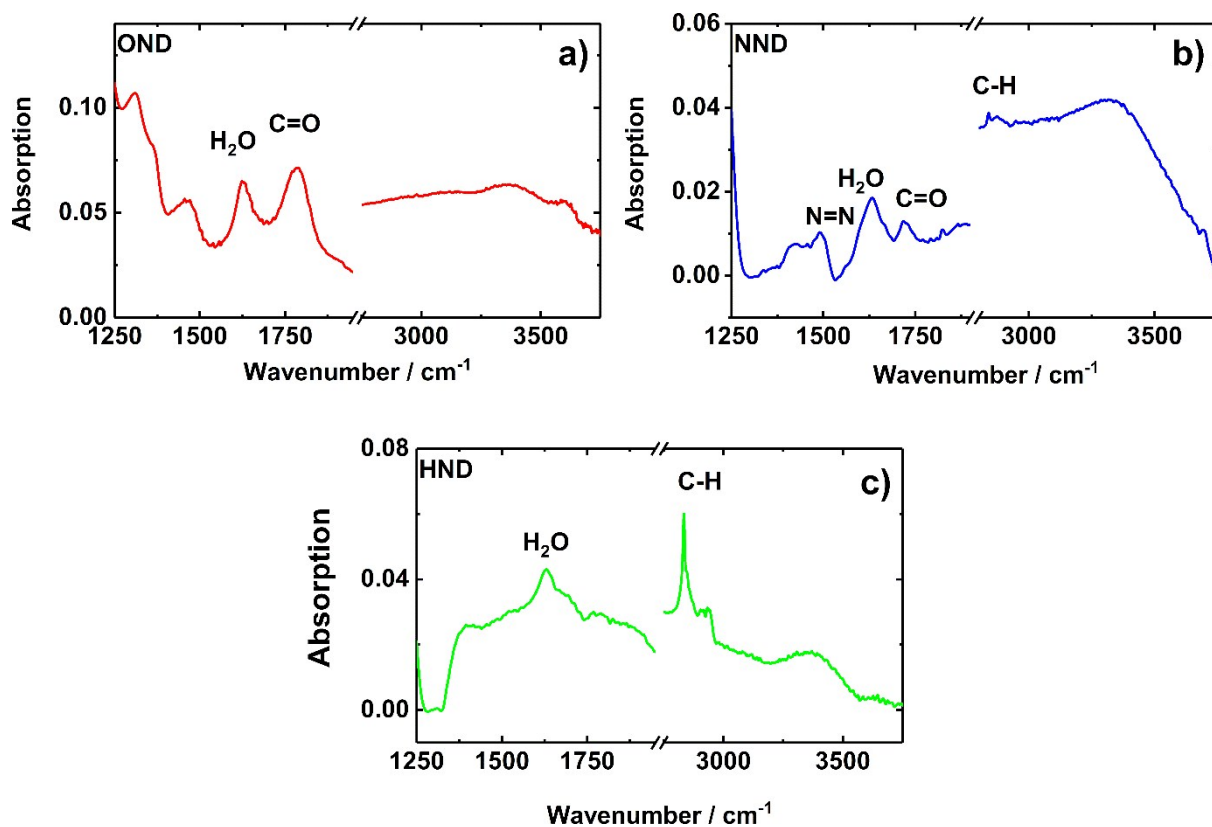


S112 Schematic illustration of band bending according to the transfer doping model for HND resulting in oxidation of the NV center: **a)** OND in contact with absorbance layer; **b)** HND in contact with absorbance layer, initializing of band bending due to electron transfer to the absorbance layer; **c)** Reduced band bending in presence of residual nitrogen acting as an electron donor; **d)** enhanced band bending resulting from the N to NV conversion. When the charge transition levels are located above the Fermi level a oxidation of the NV center appears.

The Surface Transfer Doping Model was originally established in order to explain the conductive behavior of hydrogenated diamonds (HND). Due to the low electron negativity of hydrogen (2.1) compared to carbon (2.5) the dipole moment at the surface induces the upwards shift of the valence band and the conduction band leading to the formation of a negative electron affinity in vacuum. When the hydrogenated diamond is exposed the atmospheric conditions the formed CO₂ containing water layer at the diamond surface may act as acceptor state for electrons from the upwards shifted valence band. This process leads to decrease of the Fermi level of the diamond until the equilibrium between the chemical potential of the absorbance layer and the fermi level is reach, and thus, an upwards band bending towards the surface, the electron depletion (hole accumulation) area, is formed.^{10, 11} As the charge transition states for NV^{-/0} and NV^{0/+}, that represent the threshold energy for the corresponding charge conversion, are bended in an analogue way a situation appears where

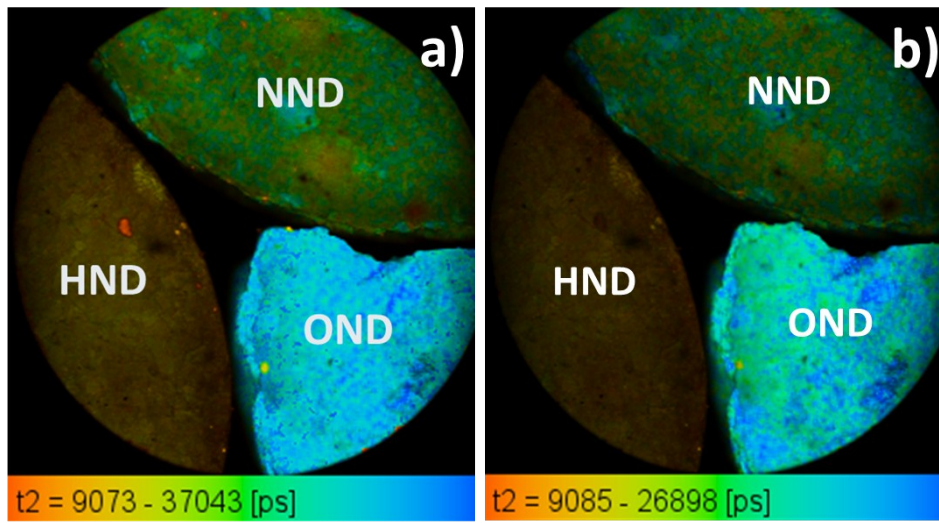
the charge transition states are located above the Fermi level. This leads to the oxidation of the NV center.^{12, 13} As the $NV^{-/0}$ charge transition states is energetically stated above the $NV^{0/+}$ charge transition states the conversion of NV^- to NV^0 is more likely to occur. The conversion of NV^0 to NV^+ leads to a fluorescence bleaching as the NV^+ is non- fluorescence.

ATR-IR spectra of the investigated NDs with different Surface Terminations



S113 ATR-IR-spectra of ND with different surface modifications: **a)** OND; **b)** NND; **c)** HND. A detailed discussion can be found elsewhere.²

Fluorescence-Lifetime Images of Pellets of NDs with different Surface Terminations



S114 Zoomed out FLIM-image ($d = 1.65$ mm) of irradiated ND-pellet ($2 * 10^{18} \text{ cm}^{-2}$) with different surface termination after excitation upon $\lambda_{\text{ex}} = 514$ nm **a)** NV^0 -channel; **b)** NV^- -channel. image

References

1. S. Ji, T. Jiang, K. Xu and S. Li, *Appl. Surf. Sci.*, 1998, **133**, 231-238.
2. C. Laube, Y. M. Riyad, A. Lotnyk, F. P. Lohmann, C. Kranert, R. Hermann, W. Knolle, T. Oeckinghaus, R. Reuter, A. Denisenko, A. Kahnt and B. Abel, *Mater. Chem. Front.*, 2017, **1**, 2527-2540.
3. F. C. Waldermann, P. Olivero, J. Nunn, K. Surmacz, Z. Y. Wang, D. Jaksch, R. A. Taylor, I. A. Walmsley, M. Draganski, P. Reichart, A. D. Greentree, D. N. Jamieson and S. Praver, *Diamond Relat. Mater.*, 2007, **16**, 1887-1895.
4. F. Jelezko and J. Wrachtrup, *Phys. Status Solidi A*, 2006, **203**, 3207-3225.
5. C. Manfredotti, S. Calusi, A. Lo Giudice, L. Giuntini, M. Massi, P. Olivero and A. Re, *Diamond Relat. Mater.*, 2010, **19**, 854-860.
6. S. Pezzagna, D. Rainer, D. Wildanger, J. Meijer and A. Zaitsev, *New J. Phys.*, 2011, **13**, 035024.
7. M. Alison and A. M. Stoneham, *J. Phys.: Condens. Matter*, 1997, **9**, 2453.
8. K. Wang, J. W. Steeds, Z. Li and H. Wang, *Appl. Phys. Lett.*, 2017, **110**, 152101.
9. P. Deák, B. Aradi, M. Kaviani, T. Frauenheim and A. Gali, *Phys. Rev. B*, 2014, **89**, 079905.
10. F. Maier, M. Riedel, B. Mantel, J. Ristein and L. Ley, *Phys. Rev. Lett.*, 2000, **85**, 3472-3475.
11. P. Strobel, M. Riedel, J. Ristein, L. Ley and O. Boltalina, *Diamond Relat. Mater.*, 2005, **14**, 451-458.
12. M. V. Hauf, B. Grotz, B. Naydenov, M. Dankerl, S. Pezzagna, J. Meijer, F. Jelezko, J. Wrachtrup, M. Stutzmann, F. Reinhard and J. A. Garrido, *Phys. Rev. B*, 2011, **83**, 081304.
13. B. Grotz, M. V. Hauf, M. Dankerl, B. Naydenov, S. Pezzagna, J. Meijer, F. Jelezko, J. Wrachtrup, M. Stutzmann, F. Reinhard and J. A. Garrido, *Nat. Commun.*, 2012, **3**, 729.